Research on mobile phone swaying and receiving position in optical camera communication[*]

JIANG Keyu, CHI Xuefen**, JI Fenglei, and LI Shuai

Department of Communications Engineering, Jilin University, Changchun 130012, China

Optical camera communication (OCC) is gaining increasing attention in researches. However, applying it to a real-world scenario may encounter many practical problems, such as the communication device may sway or there may be a position offset between the camera and the light source, which may distort the stripes and make the message unreceivable. To this end, we propose pilot-based stripe area estimation (P-SAE) decoding algorithm, and design a pixels rearrangement (PR) scheme and stripes separation logic decision method (SSLD) to improve the decoding performance under sway or receiving position offset. Finally, we build a practical OCC system and carry out experiments to verify the effectiveness of the decoding algorithm. Experimental results show that the lightweight decoding algorithm can resist the impact of smartphone sway and receiving position offset on decoding accuracy.

With the gradual advances of complementary metal-oxide-semiconductor-based (CMOS-based) camera, employing mobile-phone embedded CMOS-based camera for visible light communication (VLC), which is also known as optical camera communication (OCC), has received much attention in both academia and industries[1]. Based on the potential and availability of OCC, the IEEE 802.15.7r1 task group as the official standard of OCC further promotes its standardization development[2]. Various OCC issues and considerations, such as data rate, perspective distortion, inter-interference, demodulation method, flickering and dimming, multi-input multi-output (MIMO), and diversity are studied[3]. One of the most considerable limitations of OCC technology is data rate which is limited by the image sensors (ISs). The data rate can be increased by using higher frame cameras, which are expensive[4], and decreasing the number of pixels occupied by each stripe, which may bring the fluctuation of gray value even more susceptible to inter-interference influence. Besides, most of the existing OCC systems assume that the terminal is stationary, the sway and different receiving position scenes are not taken into account in their experiment, users may be in a complex scenario, which may cause the camera cannot recover the intended data[5]. Under this circumstance, the stripes image may be distorted, or the position of the light emitting diode (LED) luminaire in the successive frame image will change with the user's movement or hand motions. In addition, inter-interference is another difficulty, which is determined by the camera setting, such as ISO and exposure time[6].

In this work, we have reconsidered the issues of sway and position offset mentioned above, we propose pilot-based stripe area estimation (P-SAE) algorithm. Different from many existing experimental scenarios, our works in more realistic indoor luminous environments (i.e., users receive data in random time and position), where the user's status and the position relative to the LED are unknown. Besides, we design a pixels rearrangement (PR) and stripes separation logic decision method (SSLD), which can assist the P-SAE algorithm to improve the decoding performance in sway or position offset. Different from the conventional demodulation method, the new scheme we propose is no longer limited to a certain row or several rows of pixel gray values, but takes the stripe area as the decision condition. Therefore, the anti-noise ability of our system will be improved and the communication requirements for users will be much reduced. After, we realize a completed OCC practical platform using LED as transmitter and a smartphone as the receiver. At the receiver end, we develop an Android application to verify the performance. On the one hand, we test the bit error rate (*BER*) of the system to verify the feasibility of the P-SAE algorithm and the applicability of actual scenarios. On the other hand, we analyze the influence of the main parameters, such as swaying speed, tilt angle, communication distance, the position offset. The experiment results have demonstrated the efficacy of the proposed scheme.

The schematic diagram of OCC system is shown in Fig.1. The transmitted data encoded by Manchester

** E-mail: chixf@jlu.edu.cn

encoding and modulated by on-off keying (OOK) are offline generated from the personal computer (PC)[7]. The driver is composed of two parts, hardware circuit and direct current (DC) power. The hardware circuit is mainly composed of three parts microcontroller, amplifying circuit, switching circuit, and DC power. The hardware circuit of the transmitter is shown in Fig.2.
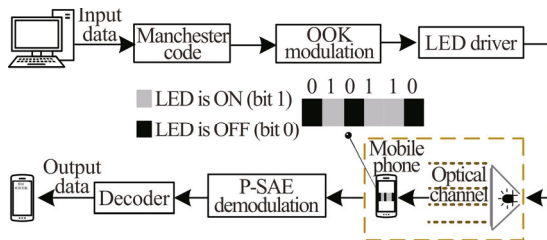

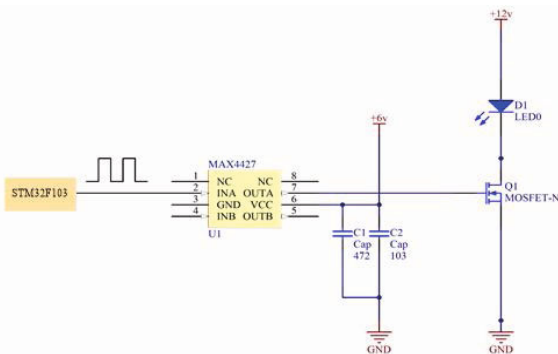**Fig.1 Schematic diagram of OCC system**

Fig.2 The hardware circuit of the transmitter

The packet structure in this paper is set according to Fig.3. Each packet has a header/pilot ('111110') and a tail ('0'). The packet sequence number (PSN) and packet synchronization symbol (PSS) follow the header/pilot and precede the payload, which occupies 5 bits. Since each packet is transmitted three times[8], the last packet data of packet N and the first packet data of packet $N+1$ may appear in one frame. Thus, PSS is proposed to distinguish the invalid frame as shown in Fig.4. The PSS of the even packet transmits '1' and the odd packet transmits '0'. If the PSS in the frame is different when the data is demodulated, the frame will be discarded.
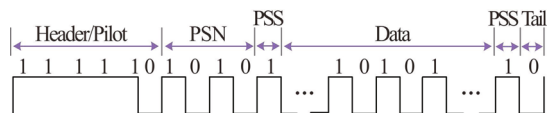

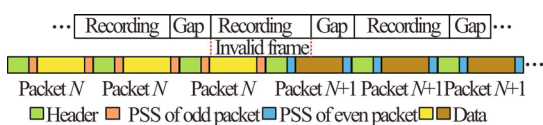**Fig.3 Schematic diagram of data packet structure**

Fig.4 Schematic diagram of PSS scheme

The sway of the smartphone and the orientation of users

relative to luminaire are important practical issues for future application of OCC. In most previous work, the camera was pointed to the LED directly to obtain data. However, this way of communication is ideal. In practical scenarios, users may be in a complex scenario where users stand in a random position or do some sway unconsciously to receive the message. As shown in Fig.5, although the image frames contain the same data, the stripe images presented are also quite different due to the difference in the degree of sway or the position offset. In previous work, the demodulation methods can be roughly divided into two categories, one is polynomial fitting based on gray value, which is easily affected by the fluctuation of gray value, the other one is demodulation based on the number of pixels of each stripe, which utilizes a fixed number of pixels to quantify all black and bright stripes. In real experiments, however, the number of pixels of each stripe is different as the inter-interference. In addition, the number of pixels in each stripe decreases with the increase of the rate, which leads to the increase of the inter-interference.
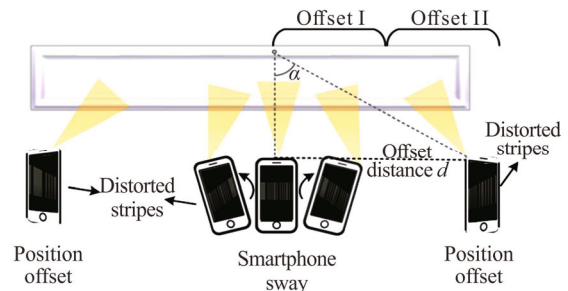

Fig.5 Illustration of mobile phone sway and positions offset

Fig.6 illustrates the flow diagram of the proposed decoding scheme. Firstly, each rolling shutter pattern frame image is extracted from a recorded video. After the grayscale transformation, all the frames are converted into grayscale values matrix. Then, the PR scheme is used to change the distortion stripes caused by sway or position offset. After PR scheme, a stripe separation scheme is proposed to avoid inter-interference. In addition, we add pilot information for two main purposes. First, it is used to quantify the stripe area and obtain the distortion characteristics of the stripe. Second, it is used to confirm the beginning of the data packet. Therefore, the next step is to find the pilot in each frame and use the P-SAE algorithm to obtain the unit stripe area for quantifying each stripe. After demodulation, we put the two pieces of data together and recover the data starting from the pilot location until a presupposed number of bits are obtained. Finally, *BER* is analyzed based on one by one check. The specific demodulation algorithm shall be shown in the next section.

The demodulation algorithm that we proposed can be divided into three parts, PR, SSLD scheme, and P-SAE algorithm. As mentioned above, the extracted images of

each frame are usually irregular shapes as shown in Fig.7(a). Ref.[9] uses a homography operation method to convert the position offset and distorted graphics into a rectangular image based on four pairs of coordinate points. However, the way to select the four points is to randomly select from the candidate matches, which means that the four pairs of point coordinates of each frame cannot be accurately obtained for the real-time changing frame image. Thus, we propose a pixels rearrangement scheme based on detecting the slope by the pilot. The application of slope detection by the pilot can assist the PR scheme to be applicable to multi-frame images that change in real-time. After PR scheme, each row of pixels is on a horizontal line and the distorted stripes have been converted into normal stripes as shown in Fig.7(b). Considering that the gray value will fluctuate with the increase of the number of stripes and the existence of inter-interference, the P-SAE algorithm based on SSLD scheme assistance is proposed as is shown in Fig.7(c). The detailed algorithm flow and will be discussed below.
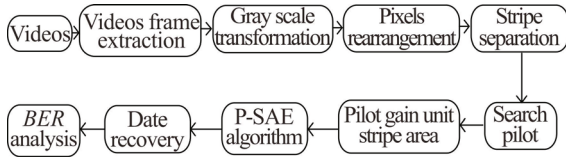

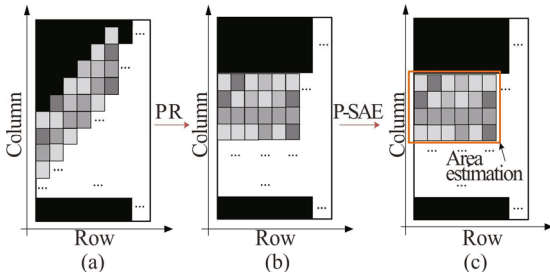**Fig.6 The offline processing of the proposed decoding scheme**

Fig.7 The schematic diagram of PR and P-SAE: (a) Original image; (b) Image after PR scheme; (c) P-SAE algorithm

Step 1: PR scheme. The proposed scheme effectively alleviates the impact of stripes distortion caused by sway or position offset as shown in Fig.7(a). The PR combined with the bilateral detection algorithm is more compatible with foreseeable scenarios. By detecting the slopes k_1 and k_2 based on pilot, we can roughly judge the user's position relative to the light source and obtain the distortion characteristics of the stripe. Then, four pairs of coordinate points need to be determined to rearrange pixels. In the selection of four pairs of coordinate points, three pairs of coordinates are available, and the other pair of coordinates needs to be specifically calculated according to the slopes. The coordinates of point 1 $I_1(x_1, y_1)$ and point 2 $I_2(x_2, y_2)$ as shown in Fig.8(a), are the corner co-

ordinates of the first strip and the last strip. The coordinates that need to be calculated are shown in Eq.(1). Note that the unfixed coordinate $I_p(x_p, y_p)$ is defined by the bilateral slope and I_1, I_2. If $k_1 < k_2$, I_3 is fixed coordinate and I_4 is determined by I_1, I_3, k_1 as shown in Eq.(2). Otherwise, I_3 is the dependent variable determined as shown in Eq.(3). After four pairs of coordinate points are determined for each frame of image, the pixels of each frame of image are rearranged to the new plane. The striped image is displayed in the new plane as shown in Fig.8(b).

$$I_p\left(x_p,y_p\right)=\begin{cases}I_4(x_4,y_4),& \text{if } k_1<k_2\\ I_3(x_3,y_3),& \text{if } k_1\geq k_2\end{cases}, \tag{1}$$

$$x_3 = x_1, y_3 = k_1\left(x_1 - x_4\right)+ y_4, \tag{2}$$

$$x_4 = x_2, y_4 = k_1\left(x_2 - x_3\right)+ y_3. \tag{3}$$
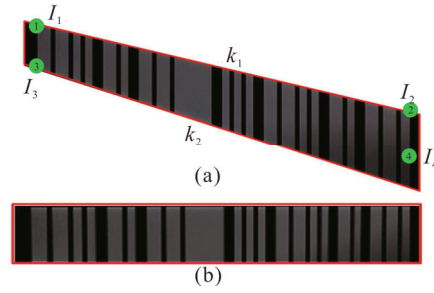

Fig.8 (a) Selection of the moving point of the distortion stripes; (b) Stripe image after PR scheme

Step 2: SSLD scheme. We define the width of bright stripe is w_1 and the width of dark stripe is w_2. Given the inter-interference, w_1 and w_2 are different. Since we adopt Manchester encoding, the bright stripes data have only three categories, '1', '11' and '11111', while the dark stripes data only have two categories, '0' and '00'. Based on the above classification analysis, we design a stripes separation logic decision scheme as shown in Fig.9. The data in the bright stripe is demodulated first, and then the data in the dark stripe is demodulated after the stripe region is de-binarized. When all the data is demodulated, data integration is performed in an alternate manner. Since the alternating feature of light and dark stripe, we use the method of separate demodulation and alternate arrangement to obtain the data information. Note that the information processed above is all that is contained in a frame of the image.

Step 3: P-SAE algorithm. Firstly, we use '111110' as the pilot, and we search for the biggest bright stripe (bright pilot). We assume that the area of bright pilot stripe is A_{pilot}. We use A_{pilot} to quantize the area of each bright stripe. The quantized formula is expressed as

$$A_{unit} = A_{pilot} / 5. \tag{4}$$

Then, we invert the binary region to decode bits '0'. We search for dark pilot B_{pilot} to quantize the area of each dark stripe. The quantized formula is expressed as
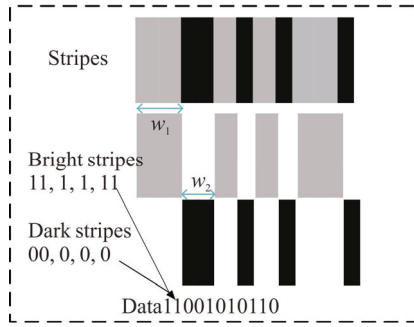
$$B_{unit} = B_{pilot}. \tag{5}$$

Fig.9 Brief schematic diagram of SSLD scheme

Finally, we use A_{unit} and B_{unit} to estimate the bit amount within the bright and dark stripe. We use Y_{nb} to represent the stripe area of n consecutive data 1, Y_{md} to represent the stripe area of m consecutive data 0. The normalized contrast is computed as follows. $Y_{1b} \approx A_{unit}$, $Y_{2b} \approx 2A_{unit}$, $Y_{5b} \approx 5A_{unit}$, $Y_{1d} \approx B_{unit}$, $Y_{2d} \approx 2B_{unit}$. Because of the inter-interference with the number of consecutive bright stripes, so we get $Y_{1b} > Y_{1d}$ and $Y_{2b} > Y_{2d}$. Following the aforementioned process, the algorithm scans each frame to obtain the area of the bright and dark stripes respectively.

In this paper, we evaluate the performance of a novel decoding algorithm through practical experiments. The specific experimental setup is shown in Fig.10 and the key experimental parameters are list in Tab.1. The transmitter includes a 70 cm×20 cm LED illuminator, STM32F103 (microcontroller, responsible for generating the information to be sent), amplifying circuit (amplifying the output signal from the microcontroller), and switching circuit (controlling the state (ON/OFF) of the luminaire). The data is generated offline from a PC. After hardware circuit loading and free-space transmission, a Nexus 5X camera APP that we develop by Android Studio is used to record and decode video. Finally, in offline processing, the captured video is loaded to the computer from the phone, and the *BER* analysis is implemented in MATLAB R2018a.
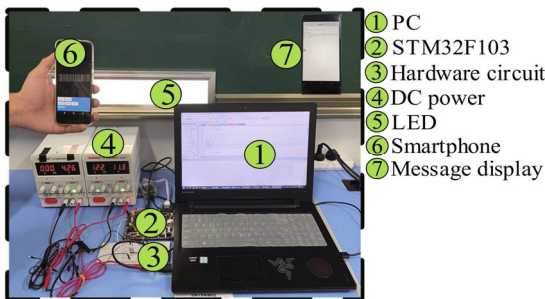

Fig.10 Experimental setup of the OCC system

We deploy a transmitter in our lab wall so that we can emulate a realistic scene. The location of the phone can be divided into two categories: the phone in front of the luminaire and the phone on the side of the luminaire.

After that, the non-static scene communication is performed by changing the position offset or swaying the phone. On the one hand, we have divided two offset levels in the communication area according to the horizontal offset distance between the phone and the center of the luminaire as shown in Fig.5, and the specific relationship between offset level and offset variable as shown in Tab.2. On the other hand, the four different swaying speeds are set to evaluate the *BER* performance of the proposed algorithm. The four different swaying speeds are 1 time/s, 2 times/s, 3 times/s, and 4 times/s. Specifically, the low swaying speed (1 time/s, 2 times/s) means slight sway unconsciously, such as user hand motions or adjusting the recording posture. A swaying speed of 3 times/s or 4 times/s means a large amount of sway, for example, the user may be in a mobile recording scene. We record video at a frame rate of 30 fps in each experiment. More importantly, in order to ensure that the phone can record the video normally, including the legible stripe image and enough information in each frame, we assume that the tilt angle shall not exceed 45° and the communication distance should be within 60 cm. Therefore, the tilt angle of the phone is randomly from −45° to 45° (negative angle means the phone is tilt to the left, while positive angle means the phone is tilt to the right).

Tab.1 Experimental parameters

Parameter	Value (Model)
Microcontroller	STM32F103
LED size	70 cm×20 cm
Output voltage	10 V
Smartphone	Nexus 5X
Resolution	1 024×768 pixels
Frame rate	30 fps
ISO	200
Exposure time	1/4 000 s

Tab.2 The specific relationship between offset level and offset variable

Offset level	Offset angle	Offset distance
I	−33°—33°	0—20 cm
II	−53°—−34°, 34°—53°	21—40 cm

Firstly, we conduct experiments under random multi-view angle offset. The user is in a random position to receive information during communication. In addition, we allow users to tilt their phones at a certain angle when receiving data. It should be noted that when receiving data, we ensure that the luminaire is always in the receiving image frame. When the voltage of transmitter is 10 V, the length of the transmitted packet is 57 bits and communication distance is 30 cm. Fig.11 illustrates *BER* performance under different tilt angles of the mobile phone in the scene of the position offset. It

can be seen from Fig.11 the *BER* stays at a low level and looks almost symmetrical. However, the *BER* increases with the increase of the offset degree. Due to the application of PR scheme and S-PAE algorithm, the *BER* increases litter with the tilt angle increases. When there is no tilt angle, the *BER* is minimum and very low. Therefore, the greater the offset level and tilt angle of the camera, the higher the *BER* of the decoding algorithm. Noted that when the tilt angle is 60°, the performance is meaningless in terms of *BER*, because compared to stripes with an angle less than 45°, the distorted stripes tend to be displayed horizontally, which can cause severe decoding failure and inability to communicate. Besides, we also tested the effect of distance on *BER* under different offset conditions. It can be seen from Fig.12 the *BER* is maintain at a low level and shows an increasing trend as the distance increases. Note that when the communication distance is greater than 40 cm, the influence of distance on the offset II will be greater than that of the offset I. We analyze the reason for this phenomenon is that as the offset and distance increase, the degree of distortion of the stripe will become larger, so the amount of change in the *BER* will increase.
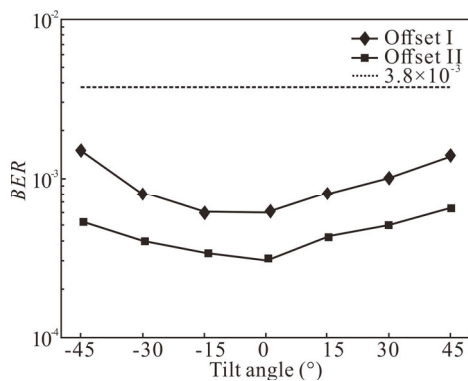

Fig.11 *BER* performance at different tilt angles in position offset scenario
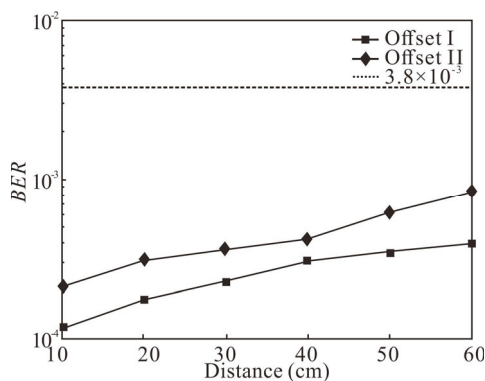

Fig.12 *BER* performance at different communication distances in position offset scenario

Secondly, the experiments are implemented under the different swaying speed of the phone. In order to simulate the practical user experience, this experiment

ensures that when the transmitter voltage is 10 V, the length of the packet is 57 bits, the communication distance are 30 cm and 60 cm, and the moving speed is 20 cm/s, the smartphone will always keep sway during video recording. The experimental results are compared with the traditional scheme based on dynamic CMS[10], as shown in Fig.13(a) and (b). It can be seen from Fig.11 that the traditional demodulation scheme is unreliable under mobile and sway conditions as a result of the instability of the phone when swaying and moving. Using the proposed decoding algorithm, the *BER* is below forward error correction (FEC) in all cases. Specifically, when the communication distance is 30 cm and the swaying speed is 1 time/s or 2 times/s, the *BER* is 1.2×10^{-4} and 1.8×10^{-4}, respectively. When we increased the swaying speed (3 times/s, 4 times/s) and set the moving speed to 20 cm/s, the *BER* increases to 9.0×10^{-4}, but it is still below the FEC limit. In addition, when the communication distance is 60 cm, the proposed system can still achieve a *BER* of 2.0×10^{-3}. It can be found that when the communication distance increases from 30 cm to 60 cm, the overall *BER* performance of the system increases. This is due to the low signal noise ratio (*SNR*) and the fluctuation of the gray value as the distance increases.
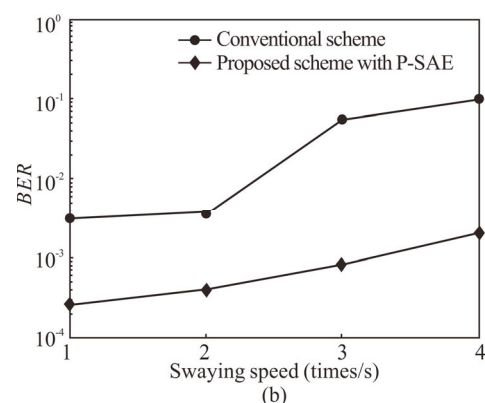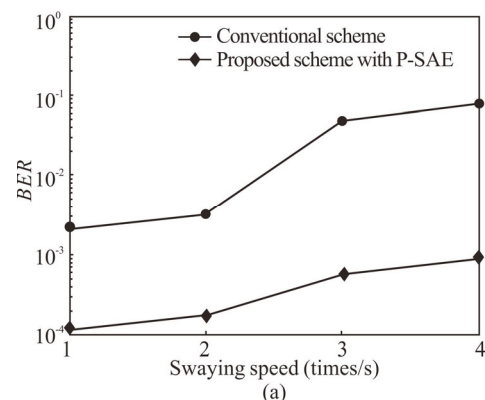

(a)

(b)

Fig.13 *BER* performance versus the swaying speed at different distances of (a) 30 cm and (b) 60 cm

In summary, the proposed P-SAE demodulation algorithm based on PR and SSLD scheme assistance is a novel and lightweight method for non-static scene OCC.

We built an actual experimental platform to verify the effectiveness and practicability of this demodulation algorithm. We analyzed the influence of external parameters when the terminal receives data, such as the swaying speed, the tilt angle, the communication distance between transmitter and receiver. In addition, internal problems at the transmitter, such as inter-interference and invalid frames, are also alleviated through our algorithm and data packet settings. Both of the experiments prove that the P-SAE demodulation algorithm based on PR and SSLD scheme assistance can resist the sway and movement of the communication devices and the impact of position offset. Further studies, informed by the work reported here, will consider OCC in long-distance swaying and moving scenarios.

Statements and Declarations

The authors declare that there are no conflicts of interest related to this article.

References

[1]   SHIVANI R T, STANISLAV Z, RAFAEL P J, et al. Spatial frequency-based angular behavior of a short-range flicker-free MIMO-OCC link[J]. Applied optics, 2020, 59(33)：10357-10368.

[2]   WANG S, CHI X F, ZHAO L L, et al. Demodulation algorithm with movement robustness for optical camera communications[J]. Optoelectronics letters, 2019, 15(6)：450-453.

[3]   NAM T L, MOHAMMAD A H, YEONG M J. A survey of design and implementation for optical camera communication[J]. Signal process：image communication,

2017, 53：95-109.

[4]   TELI S R, MATUS V, ZVANOVEC S, et al. Optical camera communications for IoT-rolling-shutter based MIMO scheme with grouped LED array transmitter[J]. Sensors, 2020, 20(12)：3361-3375.

[5]   HOSSAIN M A, ISLAM A, YEONG M J. Effects of viewing angle between camera and display in invisible image sensor communication[C]//International Conference on Information and Communication Technology Convergence (ICTC), October 19-21, 2016, Jeju, Korea (South). New York：IEEE, 2016：1221-1223.

[6]   YANG Y B, HAO J, LUO J. CeilingTalk：lightweight indoor broadcast through LED-camera communication[J]. IEEE transactions on mobile computing, 2017, 16(12)：3308-3319.

[7]   LI T Y, CHI X F, SHI H Y, et al. Rolling shutter aided optical camera communications with increasing communication distance[J]. Optoelectronics letters, 2019, 15(5)：0364-0367.

[8]   YU K, HE J, ZHENG H. A decoding scheme based on CNN for mobile optical camera communication[J]. Applied optics, 2020, 59(23)：7109-7113.

[9]   VINCENT E, LAGANIERE R. Detecting planar homographies in an image pair[C]//Proceedings of the 2nd International Symposium on Image and Signal Processing and Analysis, in conjunction with 23rd International Conference on Information Technology Interfaces, June 19-21, 2001, Pula, Croatia. New York：IEEE, 2001：182-187.

[10]   SHI J, HE J, JIANG Z W, et al. Enabling user mobility for optical camera communication using mobile phone[J]. Optics express, 2018, 26(17)：21762-21767.